EXPERIMENTAL INVESTIGATION OF THE HEAT EXCHANGE IN SEPARATION ZONES AHEAD OF CYLINDRICAL OBSTACLES

B. E. Luzhanskii and V. P. Solntsev

UDC 536.244:532.517.4

Results of an experimental investigation of the heat exchange in turbulent boundary layer separation zones ahead of cylindrical obstacles at a subsonic air stream velocity are elucidated. The investigation was conducted for changes in the ratio between the obstacle diameter and altitude between 0.25 and 4, between the boundary layer thickness at the separation point and the obstacle altitude between 0.09 and 0.7, between the Reynolds number computed by means of the free stream parameters and the obstacle height between 10^4 and $4 \cdot 10^5$. The Mach number reached 0.85. The temperature factor was 0.7. It is shown that the distribution of the heat transfer coefficients in the separation zone depends on the Reynolds and Euler numbers, the ratio between the boundary layer displacement thickness and the diameter (or altitude) of the obstacle, and the ratio between the diameter and the altitude. Criterial dependences are obtained which extend the heat-exchange results at characteristic points of the separation zones, as are also dimensionless distributions of the heat transfer coefficients to determine the heat fluxes on a plate in the plane of symmetry of the separation zone ahead of obstacles.

1. The heat exchange on the surface of bodies of complex shape with obstacles is connected with boundary layer detachment and the formation of separation zones. The results of investigating the heat exchange in two-dimensional separation zones ahead of obstacles at subsonic stream velocity have been elucidated in [1]. The flow in three-dimensional turbulent boundary layer separation zones ahead of obstacles in the shape of cylinders, rectangular parallelepipeds, and screens was investigated in [2]. Presented there are data on the flow diagrams and the characteristic dimensions of the separation zones. Some results of investigating the heat exchange in three-dimensional separation zones formed during turubulent boundary layer detachment ahead of obstacles mounted on a plate are elucidated herein.

The experiments were conducted in a subsonic wind tunnel with open working section. The experimental section was a plate 350 mm wide and 700 mm long on which cylindrical obstacles of diameter D between 30 and 120 mm and altitude H = 30 mm were mounted. The obstacle altitude was H = 120 mm for $D^\circ = D/H = 0.25$. The turbulent boundary layer thickness in the plane of symmetry of the separation section ahead of the obstacle δ varied between 2.7 and 20 mm.

The heat exchange was investigated by a method based on the theory of a regular mode of the first kind. Packets of 31 and 20 flat copper calorimeters 5 mm wide and from 1 to 5 mm thick were arranged in the plane of plate symmetry. The change in calorimeter temperature was determined on OT-24 oscillographs.

Results of investigating the flow in the neighborhood of obstacles, which included flow visualization on the obstacle and plate surfaces and determination of the characteristic dimensions of the separation zones and distributions of the static pressure and boundary layer parameters in the separation section ahead of the obstacle, were used to analyze and extend the heat-exchange data.

The flow diagrams in the three-dimensional separation zones, manifested as a result of the investigation (see [2]), are shown in Fig. 1. The turbulent boundary layer separates from the plate on the separation line 1 and attaches to the frontal surface of the obstacle at the spreading line or point 2 to form a three-

Moscow. Translated from Zhurnal Prikladnoi Mekhaniki i Tekhnicheskoi Fiziki, No. 6, pp. 83-89, November-December, 1972. Original article submitted May 10, 1972.

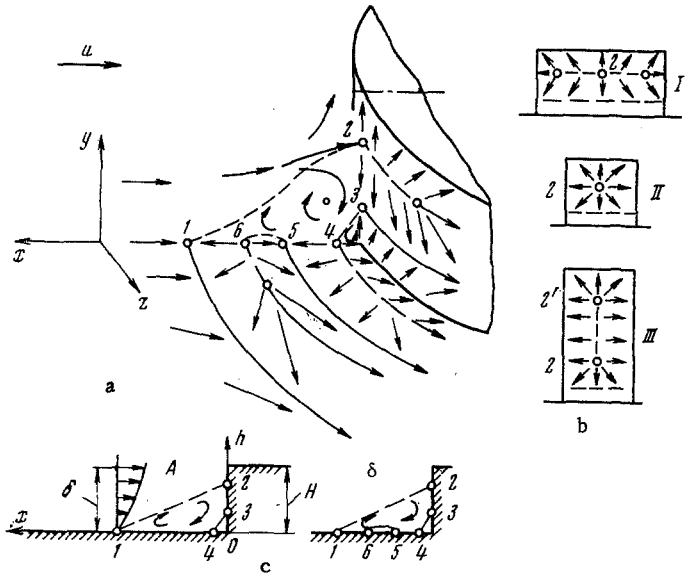

Fig. 1

dimensional separation zone ahead of the obstacle. Stream reattachment at the frontal surface of the obstacle occurs according to scheme I (Fig. 1b) for slight three-dimensionality of the flow in the separation zone, with the formation of a spreading line analogous to the spreading line in the case of two-dimensional flow ahead of an obstacle. Schemes II or III are realized for large three-dimensionality of the flow, with the formation of the spreading point 2 or the spreading line 2-2'.

The flow in the plane of symmetry is accomplished according to two schemes which agree with the flow schemes in two-dimensional separation zones ahead of an obstacle (Fig. 1c). One additional circulation zone is observed in the separation zone for a type A flow, which is formed upon detachment of the near-wall boundary layer on the separation line 3 and reattachment to the plate on the spreading line 4. Still another circulation zone exists in addition to the zone 3-4 for a type B flow when the near-wall boundary layer detaches on the line 5 and reattaches to the plate on the spreading line or point 6.

The flow picture in the neighborhood of the obstacle is determined by the parameters D°, δ^*/H and depends, as in the two-dimensional flow case, on the Euler $E = p/\rho u^2$ and Reynolds $R = uH\rho/\mu$ or $R' = uD\rho/\mu$ criteria, where δ^* is the boundary layer displacement thickness in the plane of symmetry at the point 1, u, ρ, p, μ are the free-stream velocity, density, static pressure, and dynamic coefficient of viscosity.

2. Typical distributions of the heat transfer coefficients α ($W/m^2 \cdot deg$) in the plane of symmetry of the separation zone are presented in Fig. 2 ($D^\circ = 2$, $\delta^*/H = 0.03$), $x^\circ = x/H$, $h^\circ = h/H$, where x and h are coordinates measured from the base of the obstacle (Fig. 1c). The experimental data corresponding to point 1 are obtained for $R = 6 \cdot 10^4$ and $E = 26$, and to point 2 for $R = 2.9 \cdot 10^5$ and $E = 0.85$.

The distribution of the static pressure coefficients

$$C = 2(p_0 - p)/\rho u^2$$

is shown in Fig. 2 for the second mode, where p_0 is the static pressure on the surface.

The strokes there denote the coordinates of the separation 1, the boundary layer reattachment 2, and spreading points 4 (see Fig. 1), manifested as a result of investigation of the flow configuration. Analysis of the experimental data showed that the distribution of the heat transfer coefficients is not self-similar in the separation zone and depends on the Reynolds and Euler numbers and on the parameters D° and δ^*/H.

Let us consider the heat flux distribution on the obstacle. For low numbers R (point 1 in Fig. 2), α diminishes monotonically in the separation zone from the spreading point 2 to the base of the obstacle. For high Reynolds numbers, say, for $R = 2.9 \cdot 10^5$ (point 2 in Fig. 2), the nature of the heat flux distribution changes and the values of α at the obstacle base exceed the values of α at the spreading point 2. This is explained by the fact that as the Reynolds number increases, a transition heat exchange mode appears in the near-wall boundary layer on the obstacle.

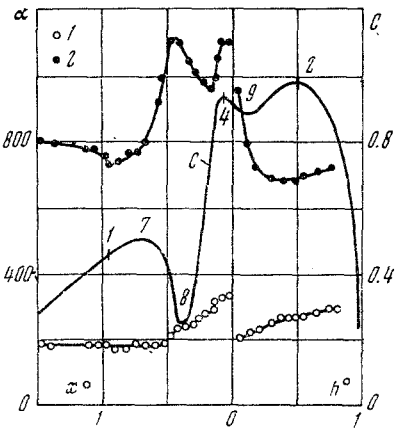

Fig. 2

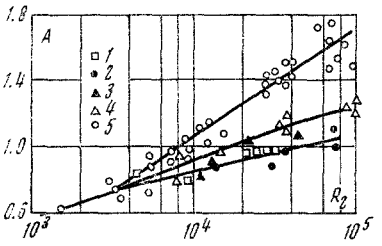

Fig. 3

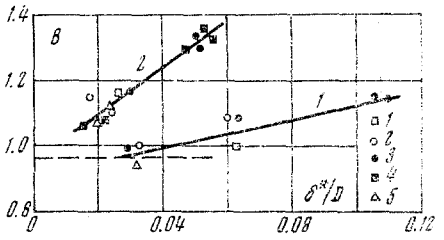

Fig. 4

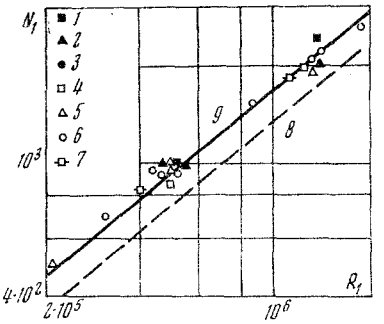

Fig. 5

The nature of the α distribution in the separation zone on the plate also depends on the Reynolds number. For low numbers R, say, for $R = 6 \cdot 10^4$ (point 1 in Fig. 2), the maximum α in the three-dimensional separation zone agrees with the spreading line 4 (Fig. 1) at the obstacle base. For high Reynolds numbers (point 2 in Fig. 2), there is a second maximum of α at the end of the accelerated portion of the flow, agreeing approximately with point 8 (Fig. 2) of the static pressure minimum on the plate in the separation zone. Criterial processing of the heat-exchange data according to local flow parameters, carried out according to the method in [3], showed that a transition from the laminar to the turbulent flow mode occurs on the accelerated flow portion from point 4 in the near-wall boundary layer. The velocity on the boundary of the near-wall boundary layer grows during flow from the spreading point 4, according to an almost power law with exponent 0.6-0.8. Hence, α diminishes on the laminar portion of the flow and increases on the turbulent portion.

It should be noted that not only an increase in the number R but also a change in Euler number and the parameters δ^*/H and D° results in analogous changes in the nature of the α distribution on a plate and obstacle if an increase in the local values of the Reynolds number in the separation zone is caused thereby.

3. The lack of self-similarity in the heat flux distribution and the difference in the heat exchange modes and the flow schemes in the separate portions of the separation zone make the computation of local values of the heat transfer coefficient in the separation zone substantially more difficult. Results of processing heat exchange data at characteristic points of the plane of symmetry of the separation zone are presented below.

Let us examine heat exchange at the spreading point 2 on the obstacle. In the case of flow according to scheme 1 (Fig. 1b), $2\ du/dh \gg du/dz$ at point 2. Processing the heat-exchange data showed that in the neighborhood of the spreading line, exactly as in the two-dimensional flow case [3], an original laminar heat-exchange mode is realized. Assuming the heat exchange at point 2 to depend on the velocity gradient analogously to the heat exchange on the spreading line of a laminar boundary layer, and taking into account that according to experimental results

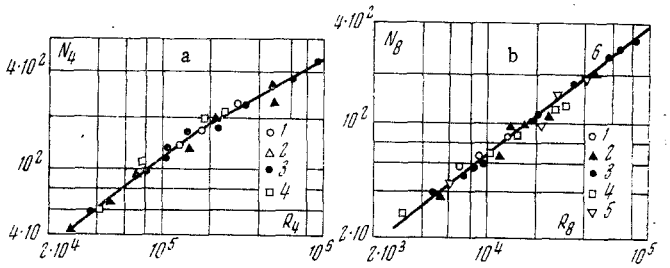

Fig. 6

$$\left(\frac{du}{dh}\right)_2 \sim \frac{u_9}{h_2} \sim \frac{u}{h_2}\left[(C_2 - C_9)\frac{\rho}{\rho_2}\right]^{0.5} \tag{3.1}$$

we can compute α_2 from the dependence

$$N_2 = AR_2^{0.5} \tag{3.2}$$

$$N_2 = \alpha_2 h_2/\lambda, \quad R_2 = uh_2\rho_2\mu^{-1}[(C_2 - C_9)\rho/\rho_2]^{0.5}$$

where u_9 is the maximum velocity on the boundary of the near-wall boundary layer on the obstacle. The subscripts 1-9 correspond to the parameters at the points denoted in Figs. 1 and 2.

The proportionality coefficient A is not a constant. Processing the data obtained, whose results are shown in Fig. 3, showed that the dependence $A = f(R, E, D^\circ, \delta^*/H)$ for obstacles of diverse geometric shape can be extended as a dependence on the number R_2 and the parameter

$$u^* = [(C_2 - C_7)/(1 - C_7)]^{0.5}$$

The parameter u^* has the meaning of a dimensionless velocity on the separating streamline in a section coincident with the point 7 (Fig. 2) of the static pressure maximum in the separation zone on the plate.

The experimental points 1 and 2 correspond to the value $u^* = 0.9$, points 3 and 4 to 0.7, and point 5 to 0.4-0.6. The points 1 are obtained when processing heat-exchange data on the frontal surface of cylindrical obstacles with $D^\circ = 4$. The remaining points are obtained when processing the authors' data on heat exchange on the frontal surface of obstacles in the shape of rectangular parallelepipeds with a ratio 2 and 4 between the width and the height (points 2 and 3, respectively) and in the case of two-dimensional flow ahead of an obstacle as δ^*/H changes from 0.06 to 0.8 (points 4 and 5). The magnitude of the temperature factor is $T_0 = 0.7$ and the Prandtl number is $\sigma = 0.7$.

As the number R_2 increases, A grows two-to threefold, which is apparently related to the influence of elevated turbulence in the separation zone on the laminar heat exchange in the neighborhood of the point 2. As δ^*/H and D° diminish, stream jets approach the spreading point 2 from domains approaching the boundary of the boundary layer, which corresponds to an increase in the parameter u^* and a diminution of the intensity of turbulence. Data on the change in $A = f(R_2, u^*)$ agree qualitatively with the data in [4] on the influence of the Reynolds number and intensity of stream turbulence on the heat exchange in the laminar portion of the accelerated flow.

Analysis of heat-exchange data on an obstacle for flows according to schemes II and III (Fig. 1b) showed that a laminar heat-exchange mode is also realized at the point 2. Hence, $(du/dh)_2 \leq (du/dz)_2$ and $(du/dz)_2 \sim u/D$ in the band of the D° and δ^* parameters investigated. In this case it is expedient to compute α_2 by means of the dependence

$$N_2' = B(R_2')^{0.5}, \quad N_2' = \alpha D/\lambda, \quad R_2' = uD\rho_2/\mu \tag{3.3}$$

A dependence of the proportionality coefficient B on the parameters D° and δ^*/D is presented in Fig. 4. The experimental points 1-5 correspond to the numbers $R' \cdot 10^{-5} = 0.7$, 1.2, 2, 4, and 9. Curve 1 averages the data obtained for $D^\circ = 1$, curve 2 for $D^\circ = 2$. The dashed line corresponds to the computed value of the coefficient B on the spreading line of an infinite cylinder streamlined transversely for $\sigma = 0.7$ and $T_0 = 0.7$. The computed value of B for a cylinder agrees well with the experimental results obtained in this wind tunnel. This indicates the absence of the influence of free stream turbulence on the spreading line of an infinite cylinder.

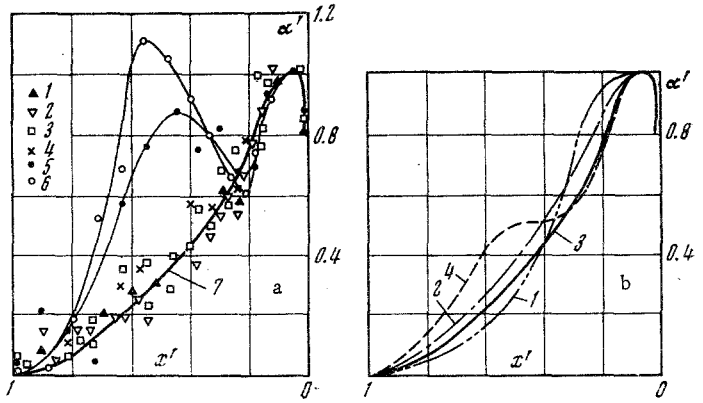

Fig. 7

In contrast to the coefficient A of the dependence (3.2), the proportionality coefficient B is independent of the Reynolds number in the range of parameters investigated. The increase in B as the parameter δ^*/D grows is related to an increase in the three-dimensionality of the flow in the neighborhood of the point 2. Thus for $D^0 = 1$ and $\delta^*/D \approx 0.04$ the scheme of the flow on the frontal surface of the obstacle is reconstructed from III to II. An increase in the parameter D° from 1 to 2 also results in a growth in the three-dimensionality of the flow at point 2 and an increase in B.

Let us examine the heat exchange at the plate at the separation 1, spreading 4 (Fig. 1), and maximum velocity points in the reverse currents zone 8 (Fig. 2).

The heat exchange at the separation point 1 can be computed by means of the dependence

$$N_1 = 0.029\, R_1^{0.8} \sigma^{0.4} T_0^{0.39} \qquad (3.4)$$
$$N_1 = \alpha_1 l_1 / \lambda_0, \quad R_1 = u_1 l_1 \rho_1 / \mu_0$$

where l_1 is an effective coordinate computed by the method in [5]. The subscript 0 refers to parameters at the wall temperature.

The computation of l_1 raises certain difficulties associated with taking account of the three-dimensionality of the flow.

Analysis showed that a simplified method can be used in a broad range of the parameters D^0 and δ^*/D to compute α_1. According to this method l_1 is computed by means of the velocity distribution on the boundary of the boundary layer without taking account of spreading, i.e., as in the case of a two-dimensional flow [5]. The influence of spreading from the plane of symmetry on the heat exchange at the point of boundary layer detachment is taken into account by using an experimental coefficient K. For the incompressible flow case the dependence for the computation of l_1 can be converted into

$$l_1 = (1 - C)^{-0.5} \int_0^{l_1} (1 - C)^{0.5}\, dl \qquad (3.5)$$

Results of processing experimental results for which l_1 was determined by means of (3.5) are shown in Fig. 5. The experimental points 1-4 have been obtained for $D^\circ = 0.25$, 1, 2, and 4, respectively, and $\delta^*/D = 0.01$-0.1. Points 5-7 have been obtained for experiments with obstacles in the shape of rectangular parallelepipeds with a width–height ratio of 1, 2, and 4. The dependence (3.4) is shown by the dashed line 8. All the data are generalized by the dependence

$$N_1 = 0.029 K R_1^{0.8} \sigma^{0.4} T_0^{0.39} \qquad (3.6)$$

where K = 1.3 (line 9) in the range of parameters investigated. In the general case, the correction coefficient K apparently depends on the parameters D° and δ^*/H. For the two-dimensional flow case ($D^\circ = \infty$) K = 1 [1].

Results of processing data on heat exchange at the points 4 (Fig. 1) and 8 (Fig. 2) are presented in Fig. 6a and b. The experimental points 1-4 correspond to the values $D^\circ = 0.25$, 1, 2, and 4, and the point 5 to the case of two-dimensional flow ahead of an obstacle. All the heat-exchange data at the spreading point 4 in the range of parameters investigated can be generalized by one curve in the coordinates

$$N_4 = \alpha_4 h_2 / \lambda, \quad R_4 = u h_2 \rho_4 / \mu$$

The analysis of experimental results on the flow portion 4-8 showed that the maximum velocity in the reverse flow zone u_8 and the coordinate x_8 can be selected as characteristic quantities governing the heat exchange at the point 8. Use of these quantities permitted generalization of the data obtained for $D^\circ = 0.25$-4 and $\delta^*/D = 0.01$-0.1, $D^\circ = \infty$ and $\delta^*/H = 0.03$-0.8, $R = 10^4 - 4 \cdot 10^5$, and $E = 0.85$-200 by the one dependence

$$N_8 = 0.04 R_8^{0.8} \quad (N_8 = \alpha_8 x_8 / \lambda, \quad R_8 = u_8 x_8 \rho_8 / \mu) \tag{3.7}$$

The criterial dependence (3.7) has been obtained for $T_0 = 0.7$, $\sigma = 0.7$. $R_8 = 3 \cdot 10^3$-10^5 and is shown by line 6 in Fig. 6b.

The lack of self-similarity in the heat flux distribution in the separation zone makes considerably more difficult the generalization of the experimental results. The distribution of the heat-transfer coefficients in the plane of symmetry of the separation zone ahead of the obstacle turned out to be represented conveniently in the coordinates

$$\alpha' = (\alpha - \alpha_1) / (\alpha_4 - \alpha_1), \quad x' = x / x_1$$

Dimensionless distributions of the heat-transfer coefficients ahead of a cylindrical obstacle for $D^\circ = 2$ are shown in Fig. 7a. The experimental points 1-6 have been obtained for $R_8 \cdot 10^{-4} = 0.3$, 0.5, 0.8, 2, 4, and 8, respectively. For $R_8 \leq 2 \cdot 10^4$, when no transition from laminar to turbulent flow occurs on the flow portion 4-8, the experimental data obtained for different values of the numbers R, E, and δ^*/D can be generalized by the single curve denoted by the solid line 7.

For other values of D° stratification of the curves $\alpha' = f(x')$ also does not occur if $R_8 < (2\text{-}3) \cdot 10^4$. Dimensionless α distributions for $D^\circ = 0.25$, 1, 2, and 4 which are independent of the number R_8 are shown in Fig. 7b by the curves 1, 2, 3, and 4, respectively.

For large numbers R_8 the α distribution in the plane of symmetry of the separation zone ahead of the obstacle can be determined by means of nomograms analogous to Fig. 7a for $D^\circ = 2$. The value α_8' can hence be used as the parameter governing stratification of the curves.

As a result of the research conducted, the heat exchange in the plane of symmetry of turbulent boundary layer separation zones ahead of cylindrical obstacles was investigated. Dependences have been obtained to compute the heat flux, in which available data on the distribution of the static pressure, velocity, and characteristic dimensions of the separation zones were used.

The authors are grateful to V. S. Avduevskii for discussing the research results.

LITERATURE CITED

1. B. E. Luzhanskii and V. P. Solntsev, "Experimental investigation of the heat exchange in turbulent boundary layer separation zones ahead of an obstacle," Zh. Prikl. Mekhan. i Tekh. Fiz., No. 1 (1971).
2. B. E. Luzhanskii and V. P. Solntsev, "Experimental investigation of the flow in three-dimensional separation zones ahead of obstacles," Zh. Prikl. Mekhan. i Tekh. Fiz., No. 1 (1972).
3. B. E. Luzhanskii, V. P. Solntsev, and V. G. Limonov, "On the question of computing the heat exchange in separation zones by using local flow parameters on the boundary of the near-wall layer," Inzh.-Fiz. Zh., 21, No. 1 (1971).
4. J. Kestin, "The effect of free-stream turbulence on heat transfer," Advances in Heat Transfer, Vol. 3, Academic Press (1966).
5. V. S. Avduevskii, "Method of computing the three-dimensional boundary layer in a compressible gas," Izv. Akad. Nauk SSSR, Mekhan. i Mashinostr., No. 4 (1962).